Mycotoxin Research (2022) 38:253–264
https://doi.org/10.1007/s12550-022-00464-0

ORIGINAL ARTICLE

Combined effects of cadmium and ochratoxin A on intestinal barrier dysfunction in human Caco-2 cells and pig small intestinal epithelial cells

So-Hee Kim[1] · Yu-Jin Jeong[1] · Min Cheol Pyo[1] · Kwang-Won Lee[1,2]

Received: 2 February 2022 / Revised: 3 July 2022 / Accepted: 19 July 2022 / Published online: 5 August 2022

Abstract

Hazardous chemicals are commonly found in cereals and cereal-based products. However, most studies focus on the individual effects of these mycotoxins or metals, rather than their combined toxicity. The main objective of this study was to evaluate the combined effects of cadmium (Cd) and ochratoxin A (OTA) on intestinal barrier integrity using Caco-2 cells and pig small intestinal epithelial (PSI) cells as models of intestinal epithelial cells and to measure alterations in cell survival and barrier integrity. The combined effects on cell viability were assessed in terms of a combination of index values. These findings showed that co-exposure to Cd + OTA had synergistic effects on Caco-2 and PSI cells at 25%, 50%, and 75% inhibitory concentrations (IC_{25}, IC_{50}, and IC_{75}, respectively) against cell viability. Individual Cd and OTA treatments had no effect, but combined Cd + OTA exposure resulted in synergistic down-regulation of paracellular apical junction complex proteins, such as claudin-1, occludin, and E-cadherin. The current findings indicate that the combined effects of OTA + Cd may have consequences at the gut level, which should not be underestimated when considering their risk to human health.

Keywords Cadmium · Ochratoxin A · Intestinal barrier · Apical junction · Synergistic toxicity

Introduction

The global average consumption of cereal-based foods reached 171 kg/person/year in 2015, continuing the current trend of stabilization until 2030 (Yang et al. 2020). Previous studies have reported the maximum levels of cadmium (Cd) in cereal samples (199 µg/39–44) (Skendi et al. 2019), and those of ochratoxin A (OTA) in cereals and cereal-based products (1164 µg/kg) (Lee and Ryu 2017) were reported (Brizio et al. 2016; Hamnér and Kirchmann 2015; Lee and Ryu 2017; Skendi et al. 2019; Yang et al. 2020). Cd is a heavy metal found naturally in soil and water that can contaminate foods (Cabrera et al. 1998; McLaughlin et al. 1999). Because of their high bioaccumulation, cereal-based products are major dietary sources of Cd (Kirkham 2006; Wang et al. 2019). Cd is absorbed orally through the gastrointestinal tract, then transported through the blood and deposited in the kidneys and liver (Norman 1992; Rana et al. 2018). The IARC classifies Cd as group 1 (carcinogenic to humans) (IARC 1993). Cd is a recognized nephrotoxic chemical that may also damage bones and the liver (Tinkov et al. 2018). The European Food Safety Authority (EFSA) has established a tolerable weekly intake (TWI) of 2.5 µg/kg body weight (b.w.) for Cd, as the standard for human exposure safety management (EFSA 2012). Cd is regulated at the level of 0.2 mg/kg by the Codex Alimentarius collection of food standards (CODEX) (FAO and WHO 2002). OTA is a

Highlights
- Combined treatment with cadmium and ochratoxin A intensifies the barrier dysfunction of intestinal epithelial cells.
- Combined treatment with Cd + OTA, at non-cytotoxic doses, synergistically induces intestinal barrier dysfunction.
- Synergistic down-regulation of claudin-1, occludin, and E-cadherin was observed following the combined treatment.
- The combined risks of OTA and Cd in the gut should not be underestimated for human health.

✉ Kwang-Won Lee
kwangwon@korea.ac.kr

[1] Department of Biotechnology, College of Life Sciences and Biotechnology, Korea University, Seoul 02841, South Korea

[2] Department of Food Bioscience and Technology, College of Life Sciences and Biotechnology, Korea University, Seoul 02841, South Korea

mycotoxin produced by various fungi of the genera *Aspergillus* and *Penicillium* and is found in cereals, meat, cheese, and dried and fresh fruits (EFSA Panel on Contaminants in the Food Chain (CONTAM) et al. 2020). In the European Union, OTA is regulated at a maximum level of 0.5–20 µg/kg in foods, including unprocessed cereals, processed cereal-based foods for infants, and all products derived from unprocessed cereals and spices (EC 2006). The IARC classifies OTA as group 2B (possibly carcinogenic to humans) (WHO and IARC 1993). The standard for human exposure safety management for OTA was set by EFSA as a TWI for OTA of 120 ng/kg b.w. (EFSA 2006).

Contaminant-induced intestinal barrier dysfunction can cause inflammatory bowel disease among other things (Groschwitz and Hogan 2009). Cd and OTA have been shown to be cytotoxic to intestinal cells. Cd (20 µmol/L) considerably lowered the viability of porcine jejunal epithelial IPEC-J2 cells after 3 h of treatment (Razzuoli et al. 2018). After 12 h of exposure to 2 µmol/L OTA, an OTA-induced cytotoxic effect was observed in IPEC-J2 cells (Wang et al. 2018). On the other hand, the apical junction complex consists of a tight junction and an apical junction and is an important factor regulating intestinal barrier function (Luissint et al. 2016). In in vitro intestinal models, Cd has been shown to increase intestinal permeability through disruption of claudin 4 (CLDN4), occludin (OCLN), zonula occludens-1 (ZO-1), and E-cadherin (Duizer et al. 1999; Rusanov et al. 2015). Cd exposure also lowers the expression of CLDN1, OCLN, and ZO-1/2 in mice, thereby increasing colon and jejunum intestinal permeability (Zhai et al. 2016). Similarly, OTA enhanced intestinal permeability in in vitro intestinal models by downregulating OCLN, CLDN, and ZO-1 (Alizadeh et al. 2019; McLaughlin et al. 2004; Romero et al. 2016).

Most research has concentrated on the individual impacts of mycotoxins or metals, rather than their combined toxicity (Luo et al. 2019). In practice, the human body is rarely exposed to either Cd or OTA on its own. Exposed to Cd and OTA occur through cereal and cereal-based products, since these are common co-contaminants of the same (Yang et al. 2020). When OTA and Cd are ingested together as dietary contaminants, their influence on human health may be changed. Little is known about the interaction of OTA and Cd with intestinal cells. The main objective of this work was to evaluate the combined effects of Cd + OTA on intestinal barrier integrity, utilizing two intestine-derived cell lines, Caco-2 and pig small intestinal (PSI) epithelial cells, as models of intestinal epithelial cells, for evaluating cell survival and barrier integrity alteration. Furthermore, the results of multiple endpoints (expression and localization of apical tight junction proteins) were analyzed to assess Cd-OTA interactions at the intestinal level.

Materials and methods

Test substances

Cadmium chloride was purchased from Merck (St. Louise, MO, USA), and OTA (CAS no. 303–47-9; > 98% purity, benzene-free solid) was obtained from Cfm Oskar Tropitzsch (Marktredwitz, Germany). Stock solutions of Cd and OTA at initial concentrations of 100 mmol/L were prepared by dissolving $CdCl_2$ (18.33 mg) in 1 mL of deionized water and OTA (40.38 mg) into dimethyl sulfoxide (DMSO, CAS no. O1877, Merck).

Cell culture and differentiation

As the absorption of Cd and OTA occurs mostly in the small intestine, the human colon carcinoma cell line (Caco-2) and PSI were used in the present study. Caco-2 cells were purchased from American Type Culture Collection (Rockville, MD, USA). The PSI epithelial cell line was provided by Prof. Wilhelm Holzapfel (School of Life Sciences, Handong University, Republic of Korea). The cells were cultured in Dulbecco's modified Eagle's medium (low glucose, Gibco, Grand Island, NY, USA) containing 3.7 g /L sodium bicarbonate, 1% (v/v) penicillin/ streptomycin, and 10% (v/v) fetal bovine serum. Additionally, the medium was supplemented with 1% (v/v) nonessential amino acids for Caco-2 cells. The cells were incubated in a humidified incubator under constant conditions (5% CO_2 and 37 ℃).

Although Caco-2 cells are colon-derived, one of the most advantageous characteristics of Caco-2 cells is that they have the capacity to spontaneously differentiate into a monolayer of cells, with several properties similar to those of absorptive enterocytes that are seen as a brush border layer seen in the small intestine (Lea 2015). Therefore, Caco-2 cells were differentiated to have small intestine cell-like characteristics in all the experiments. However, in terms of pathology, physiology, and anatomy, in addition to weight, size, and sensitivity toward OTA, pigs are comparable to humans (Jørgensen and Petersen 2002). PSI cells have non-carcinoma, untransformed features, similar to those of primary small intestinal cells (Trapecar and Cencic 2012). In several studies, the effect of OTA has been evaluated using porcine-derived intestinal cells (Wang et al. 2018). PSI cells, which are small intestine-derived cells, were used without differentiation in the present study.

For monolayer formation, cells were seeded on 12-well inserts (Falcon, Oxnard, CA, USA) at a density of 5.4×10^4 cells/cm^2 for Caco-2 and 1.4×10^4 cells/cm^2 for PSI. Caco-2 and PSI cells were incubated for 15–21 d, with the medium replaced every 2 or 3 d (Alizadeh et al. 2019; Lee et al. 2018b). The trans-epithelial electrical resistance (TEER)

value was measured every three days, for 21 d, and compared to the TEER values considered to be stably polarized in previous studies. The period and TEER values with the highest and most stable values were selected. The TEER value was measured 15 d after seeding, and when it reached a certain level, the experiment was performed. In the Caco-2 cell model, cells were differentiated for 21 d. In the TEER and permeability experiments, PSI cells were cultured for 15–21 d. In all experiments, Caco-2 cell monolayers with TEER > 400 $\Omega \times cm^2$ were used, as previously described (Cilla et al. 2018). PSI cell monolayers with TEER > 350 $\Omega \times cm^2$ were used for TEER and permeability experiments.

Cadmium chloride was purchased from Merck and was dissolved into distilled water. OTA was purchased from Cfm Oskar Tropizch (Marktredwitz, Germany) and dissolved in DMSO.

Cell viability analysis

Cell viability was measured using the 3-(4,5-dimethylthiazol-2-yl)-2,5-diphenyltetrazolium bromide (MTT) assay. Caco-2 cells were seeded in 24-well plates, at a density of 5.4×10^4 cell/cm^2, and differentiated for 21 d, followed by treatment with Cd and OTA for 48 h. The PSI cells were seeded into 24-well plates, at a density of 2.0×10^4 cell/cm^2, and incubated for 24 h, followed by treatment with Cd and OTA for 48 h. Next, MTT (5 mg/mL in distilled water) was diluted fivefold in the medium, to a concentration of 1 mg/mL, before being used. The MTT solution was added to the wells and incubated for 3 h. Next, in order to dissolve insoluble formazan, the MTT solution was removed, followed by the addition of DMSO. Finally, the absorbance was measured at the wavelength of 540 nm, using a microplate reader (EL-808, Bio Tek, Winooski, VT, USA).

TEER measurement

To measure TEER, we used an ohm/voltmeter (EVOM, WPI, Sarasota, FL, USA) containing Hank's balanced salt solution supplemented with $NaHCO_3$. TEER values were calculated by using the following formula:

$$TEER\left(\Omega/cm^2\right) = \left(R_{\text{total}} - R_{\text{blank}}\right) \times \text{Area of membrane } \left(cm^2\right)$$

The TEER was measured before and after treatment. The results are presented as a percentage of the final value to the initial value.

Fluorescein isothiocyanate-dextran flux assay

Paracellular permeability was determined by measuring the flux of fluorescein isothiocyanate (FITC)-dextran (4 kDa; Merck) in Caco-2 and PSI cell monolayers. After treatment, 1 mg/mL FITC-dextran 4 kDa was added to the apical side and incubated for 2 h at 37 ℃. Samples were collected from the basolateral side, and fluorescence was measured using a fluorometer (HIDEX, Turku, Finland) at wavelengths of $\lambda_{ex} = 488$ nm and $\lambda_{em} = 525$ nm. The FITC-dextran flux was expressed as the permeability coefficient (Papp). *Papp* was calculated using the following formula:

$$Papp\ (cm/s) = \left(\frac{V_A}{A \times t}\right) \times \left(\frac{C_f}{C_i}\right)$$

where *Papp* is the permeability coefficient, V_A is the volume (cm^3) of the receiver (basolateral side), C_f is the concentration (μmol/L) of the receiver (basolateral side), A is the surface of the filter (cm^2), t is the assay time (s), and C_i is the initial apical concentration (μmol/L).

Isobologram method for assessing the combined effects of Cd + OTA

The interaction was quantified using the Chou and Talalay method (Chou 2010). The combination index (CI) value was calculated using the following formula:

$$^{n}(CI)_x = \sum_{j=1}^{n} \frac{(D)j}{(Dx)j} = \sum_{j=1}^{n} \frac{(D_x)_{1-n}\left\{[D]_j / \sum_1^n [D]\right\}}{(D_m)_j \left\{(f_{a_x})_j / 1 - (f_{a_x})_j\right\}^{1/m_j}}$$

where $^{n}(CI)_x$ is the combination index for n contaminants at x% effect, D is the concentration of the contaminant, $(D_x)_{1-n}$ is the sum of n contaminants that exerts x% effect in combination, $[D]_f / \sum_1^n [D]$ is the proportionality of each of n contaminants that exerts x% effect in combination, and $(D_m)_j \left\{(f_{a_x})_j / [1 - (f_{a_x})_j]\right\}^{1/m_j}$ is the concentration of each contaminant alone that exerts the x% effect. D_m is the median-effect dose [antilog of the x-intercept (r) of the median-effect plot], and m is the slope of the median-effect plot that depicts the shape of the dose–effect curve. $m = 1, > 1$, and < 1 indicates, hyperbolic, sigmoidal, and flat sigmoidal curves, respectively, and f_{a_x} is the fraction inhibition of the x% effect. A CI < 1 indicates a synergistic effect, while CI = 1 indicates an additive effect, and CI > 1 indicates an antagonistic effect. The IC_{25}, IC_{50}, and IC_{75} values represent the concentrations that inhibit cell viability by 25%, 50%, and 75%, respectively.

CompuSyn software version 1.0 (ComboSyn Inc., Paramus, NJ, USA) was used to generate the dose–effect relationship analysis, median-effect dose, and percentage affected-combination index (*fa-CI*) plot. The dose–effect parameters (D_m, m, and r) were considered by using the median-effect dose (m), where r is the linear correlation coefficient of the median-effect plot. CI values were calculated by the *fa-CI* plot.

Quantitative real-time PCR analysis

Total RNA was isolated using RNAiso PLUS (Takara, Kusatsu, Japan). RNA concentration and purity were measured using a NanoDrop™ 2000 system (Thermo Scientific, IL, USA). First-strand cDNA was synthesized in accordance with the instructions of the Premium Express 1st strand cDNA synthesis system (LeGene Biosciences, San Diego, CA, USA). Quantitative real-time PCR analysis (qRT-PCR) was performed with SYBR® Green (Elpis Biotech Inc., Daejeon, South Korea) on a CFX96™ Real-Time PCR system (Bio-Rad Laboratories, Inc., Hercules, CA, USA). Primers used in this study are listed in Supplementary Table S1.

Western blot

Radioimmunoprecipitation assay (RIPA) buffer (EBA-1149, Elpis Biotech Inc.) was used to extract proteins from cells. RIPA buffer consisted of 50 mM NaCl/50 mM Tris–HCl (pH 7.5), 0.2% deoxycholic acid/0.5% Triton X-100™/1% Nonidet P-40 containing 0.1%, and 1 mM phenylmethylsulfonyl fluoride, in the presence of aprotinin and leupeptin. The supernatant obtained by means of centrifugation (13,793 × *g* for 20 min) was used as the total cell lysate. Protein samples were separated on SDS–polyacrylamide gels and transferred to Immnobilion®-P transfer membranes (Millipore, Billerica, MA, USA). Proteins were detected using primary antibodies, GAPDH (sc-32233, Santa Cruz Biotechnology, TX, USA), claudin-1 (sc-166338, Santa Cruz Biotechnology, Dallas, TX, USA), claudin-4 (sc-376643, Santa Cruz Biotechnology), occludin (sc-271842, Santa Cruz Biotechnology), ZO-1 (13663S, Cell Signaling Technology, Danvers, MA, USA), and E-cadherin (14472S, Cell Signaling Technology for Caco-2 cells; sc-8426, Santa Cruz Biotechnology for PSI cells), and then incubated with the appropriate secondary antibodies. Finally, the proteins were detected using an Amersham ECL Select™ reagent kit (GE Healthcare, Chicago, IL, USA). Signal intensity was quantified using ImageJ software (National Institutes of Health, Bethesda, MD, USA).

Immunofluorescence

The localization of the tight junction proteins was measured by means of immunofluorescence staining in differentiated Caco-2 cells and undifferentiated PSI cells. The cells were seeded onto 13-mm confocal dishes (200,350, SPL Life Sciences Co., Ltd., Pocheon, South Korea) at a density of 5.4×10^4 cell/cm^2 for Caco-2 cells and 2.0×10^5 cell/cm^2 for PSI cells. Differentiated Caco-2 and PSI cells were treated with Cd and OTA. Next, 4% paraformaldehyde was added to the wells, followed by the addition of 0.1% Triton™ X-100, for fixation and permeabilization, respectively. Following that, the cells were incubated with 1% bovine serum albumin for 1 h. The cells were then incubated with a primary antibody at 4 ℃ overnight, followed by incubation with a secondary antibody (Abcam Inc., Cambridge, CA, USA) for 2 h. Nuclei were stained using a 4′, 6-diamidino-2-phenylindole (DAPI) solution of concentration 500 ng/mL for 10 min. The localization of CLDN1, OCLN, and ZO-1 was observed using a confocal laser-scanning microscope (CLSM 700, Carl Zeiss, Oberkochen, BA, Germany).

Data and statistical analysis

Data are expressed as the mean ± standard deviation values. All experiments were repeated 3 times, and each experiment was performed in triplicate. Differences were considered statistically significant at $p < 0.05$. Different letters indicate significant differences, as assessed using analysis of variance (ANOVA), followed by Tukey's multiple range test. All statistical analyses were performed using SAS version 9.4 software (SAS Institute, Cary, NC, USA). TEER, permeability, PCR, and western blot data were analyzed as previously described (Li et al. 2017). The type of interaction was determined by comparing the "measured values (M)" defined as examined endpoints to the "expected values (*E*)" defined as the sum of toxic effect values induced by a single treatment. *E* was calculated using the following formulae:

$$E = C_{mix} - \left(C_a - M_a\right) - \left(C_b - M_b\right) \text{ (when, } M < C\text{)}$$

$$E = C_{\text{mix}} + \left(M_a - C_a\right) - \left(M_b - C_b\right) \text{ (when, } M > C\text{)}$$

In the co-exposure treatments, the C_{mix} reflects the outcome of the control groups. In the *a*/*b* mono-exposure treatments, C_a and C_b reflect the outcomes of the control groups, while M_a and M_b reflect the outcomes of the treated groups.

The significance of the difference between the measured and expected values was assessed using one-way ANOVA to determine whether there was an interaction. If the *p*-values were less than 0.05, the results were considered significant and an interaction effect (synergic or antagonist effect) was assumed; otherwise, an additive effect was assumed.

Results

Individual and combined cytotoxic effects of Cd + OTA in Caco-2 and PSI cells

To assess the toxicity induced by co-contamination with Cd and OTA, the outcomes of the analysis of the Cd and OTA content that could be obtained from cereal and cereal-based product samples were used. Yang et al. (2020) investigated

Cd and OTA levels in samples of cereal and cereal-based products from China in 2010. The molar ratio (Cd/OTA) determined by referring to the mean values in the results of this study, *i.e.*, Cd (17.6 µg/kg or 0.157 µmol/kg) and OTA (94.2 µg/kg or 0.233 µmol/kg), was 1/1.5. Based on these findings, the Cd/OTA concentration ratio used in the MTT assay was set to 1:1.5 in the present study. At various concentrations, a combination of the constant ratio (Cd/OTA = 1/1.5) was applied for 48 h to evaluate the interaction between Cd and OTA in differentiated Caco-2 cells and PSI cells without differentiation using the MTT assay (Fig. 1). The type of interaction was evaluated in terms of *fa-CI* plot and CI values obtained using the CompuSyn software program (Supplementary Fig. S1).

As shown in Fig. 1a, Caco-2 cell viability was higher than 80% at Cd and OTA concentrations in the ranges of 0–2.0 µmol/L and 0–3.0 µmol/L, respectively, which suggested that these concentrations were non-cytotoxic. According to the Chou and Talalay method, these results showed that Cd + OTA have a toxic effect of common synergism at IC_{25} (*0.38137*), IC_{50} (*0.33759*), and IC_{75} (*0.31695*) against cell viability of Caco-2 (Supplementary Table S2). The CI value was the lowest at concentrations of 2.0 µmol/L Cd and 3.0 µmol/L OTA, with *fa* of *0.2077* and CI of *0.23411* (strong synergism), resulting in > 80% cell viability in Caco-2 (Supplementary Table S3).

Similarly, PSI cell viability was higher than 80% at Cd and OTA concentrations in the ranges of 0–0.4 µmol/L and 0–0.6 µmol/L, respectively, which meant that these concentrations were non-cytotoxic (Fig. 1b). Cd + OTA had a toxic effect with moderate synergism at IC_{25} (*0.81574*) and common synergism at IC_{50} (*0.64646*) and IC_{75} (*0.51817*) in PSI (Supplementary Table S2). Although the CI value (*0.31815*) was the lowest at concentrations of 4.0 µmol/L Cd and 6.0 µmol/L OTA, and the *fa* value was *0.9457*, there was a reduction in cell viability by 95% in PSI (Supplementary Table S3). Therefore, a concentration of Cd (0.4 µmol/L) and OTA (0.6 µmol/L), with *fa* of *0.1767* and CI of *0.79942* (moderate synergism), resulting in ≥ 80% cell viability, was selected for the PSI cells. Taken together, we chose the concentrations of 2.0 µmol/L Cd + 3.0 µmol/L OTA and 0.4 µmol/L Cd + 0.6 µmol/L OTA for treating Caco-2 and PSI, respectively, in the further experiments.

Individual and combined effects of Cd and OTA on intestinal barrier function in Caco-2 and PSI cells

To assess intestinal barrier function, we evaluated the effects of Cd (2 µmol/L in Caco-2 cells and 0.4 µmol/L in PSI cells) and OTA (3 µmol/L in Caco-2 cells and 0.6 µmol/L in PSI cells), individually and in combination, on TEER and FITC-dextran 4 kDa flux of Caco-2 and PSI cell monolayers. As shown in Fig. 2a, TEER values of the control, Cd, OTA, and Cd + OTA groups in Caco-2 cells were 38%, 30%, 26%, and 4%, respectively, relative to the initial baseline TEER value. In Caco-2 cells, Papp was 0.28 cm/s, 0.35 cm/s, 0.40 cm/s, and 1.13 cm/s in the control, Cd, OTA, and Cd + OTA groups, respectively (Fig. 2b). As shown in Fig. 2c, the TEER values of the control, Cd, OTA, and Cd + OTA groups were 59%, 65%, 60%, and 54%, respectively, compared

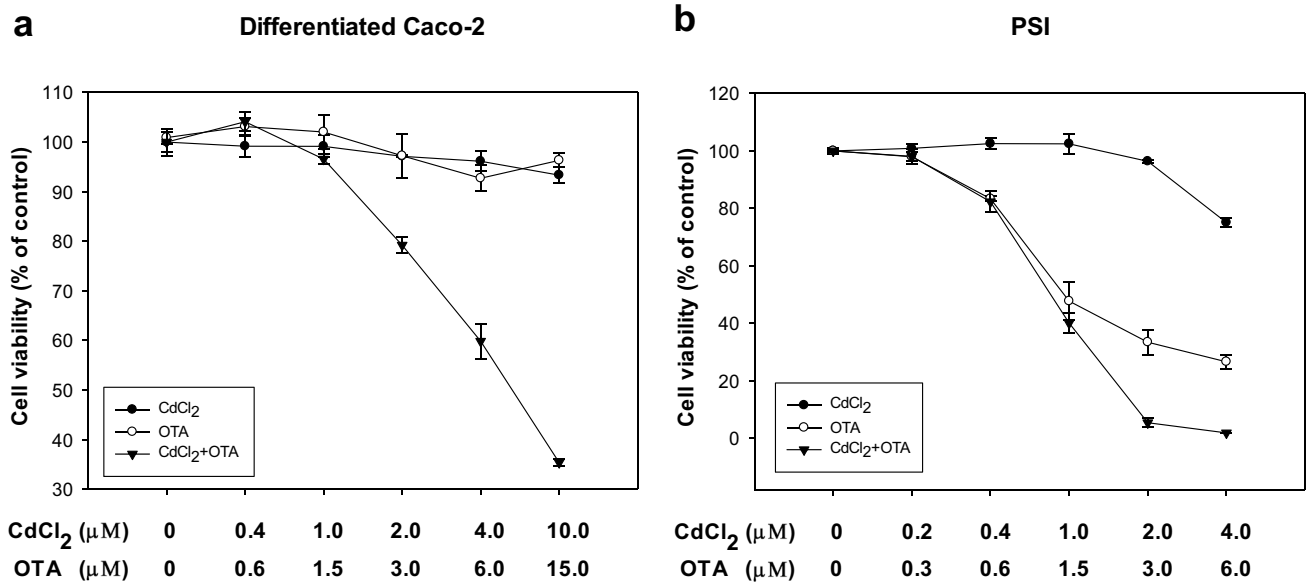

Fig. 1 Individual and combined cytotoxic effects of Cd and OTA in (**a**) differentiated Caco-2 and (**b**) PSI Cells. Cell viability was assessed using MTT assay. Caco-2 cells were treated to different concentrations of $CdCl_2$ (0.4 µmol/L, 1 µmol/L, 2 µmol/L, 4 µmol/L, 10 µmol/L) and OTA (0.6, 1.5, 3, 6, 15) for 48 h. PSI cells were treated to different concentrations of Cd (0.2 µmol/L, 0.4 µmol/L, 1.2 µmol/L, and 4 µmol/L) and OTA (0.3, 0.6, 1.5, 3, and 6) for 48 h

with the initial value in PSI cells. In PSI cells, the Papp was 0.74 cm/s, 0.71 cm/s, 0.94 cm/s, and 1.61 cm/s in the control, Cd, OTA, and Cd + OTA groups, respectively (Fig. 2d). In Caco-2 and PSI cells, the TEER values were not significantly ($p < 0.05$) higher in the groups treated individually with Cd or OTA than in the combined Cd + OTA-treated group (Fig. 3). However, the TEER value was significantly ($p < 0.05$) lower in the Cd + OTA-treated group than that in the control group. Based on the formula in the "Data and statistical analysis" section, the combined treatment showed an additive effect on the TEER value [measured value (M) = 4.40 *vs*. expected value (E) = 18.4; $p > 0.05$] in Caco-2 cells and a synergistic effect (M = 65.4 *vs*. E = 54.5; $p < 0.05$) in PSI cells.

In Caco-2 and PSI cells, paracellular permeability of all groups was significantly ($p < 0.05$) higher than that of the control in all groups, except in the case of the Cd group in PSI cells (Fig. 4). The combined treatment showed a synergistic effect because M was significantly higher than E in Caco-2 cells (M = 0.225 *vs*. E = 1.13; $p < 0.05$) and PSI (M = 0.496 *vs*. E = 1.51; $p < 0.05$) cells. Therefore, combined treatment with Cd + OTA synergistically reduced intestinal permeability.

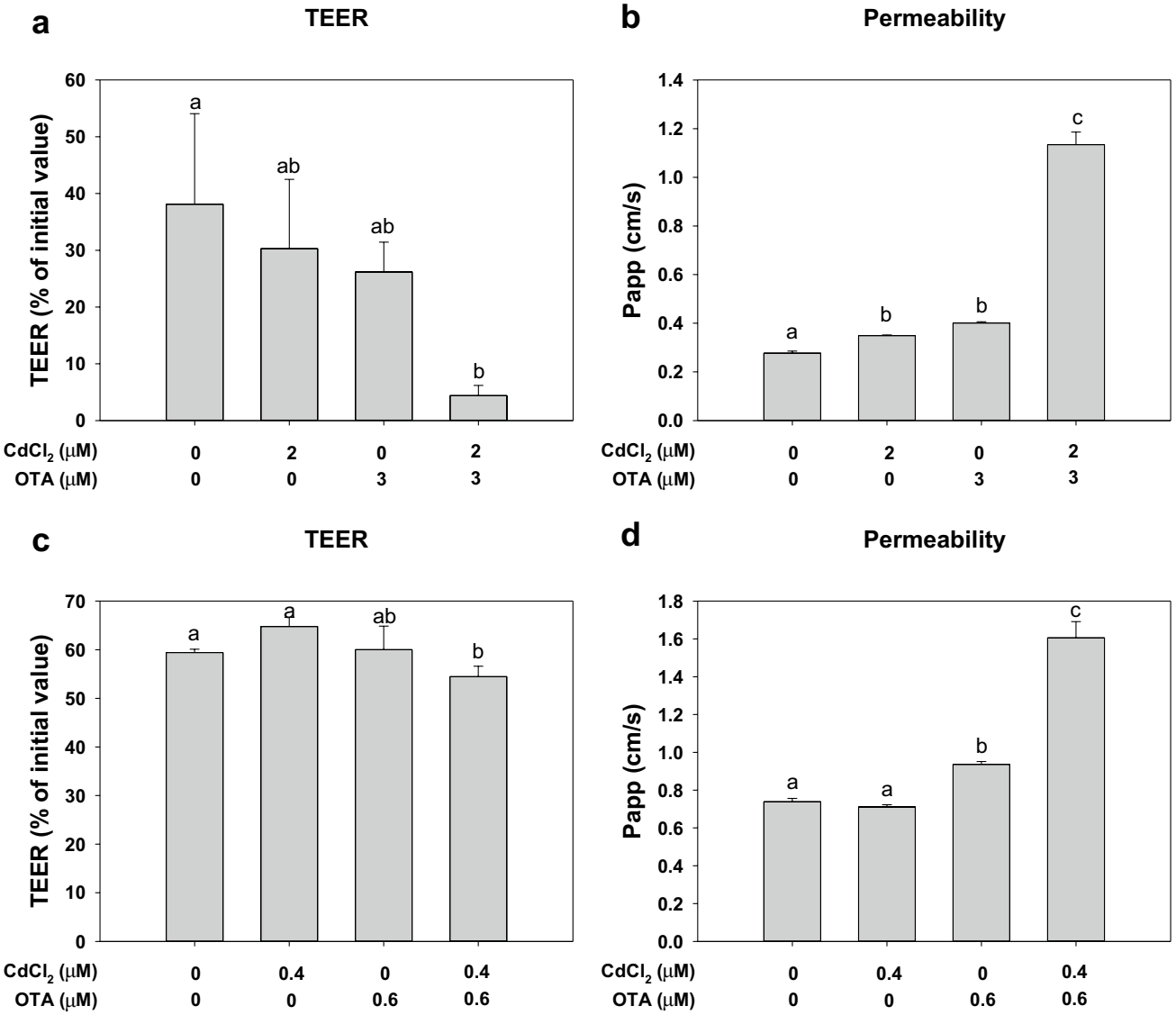

Fig. 2 Individual and combined effects of Cd and OTA on TEER and the paracellular permeability in differentiated Caco-2 (**a** and **b**) and PSI (**c** and **d**) cells. Caco-2 cells were differentiated on an insert and treated to on the apical side with $CdCl_2$ (2 µmol/L) and OTA (3 µmol/L) for 48 h. PSI cells were treated with $CdCl_2$ (0.4 µmol/L) and OTA (0.6 µmol/L) for 48 h. The permeability coefficient (Papp) was determined, with the paracellular flux of fluorescein isothiocyanate (FITC)-dextran 4 kDa from the apical to the basal side. The results are presented as a percentage of the initial value, in terms of mean ± standard deviation (S.D.) of 3 independent experiments. Different letters (**a**, **b**, **c**, and **d**) indicate significant differences at $p < 0.05$ as assessed using ANOVA followed by Tukey's multiple range tests

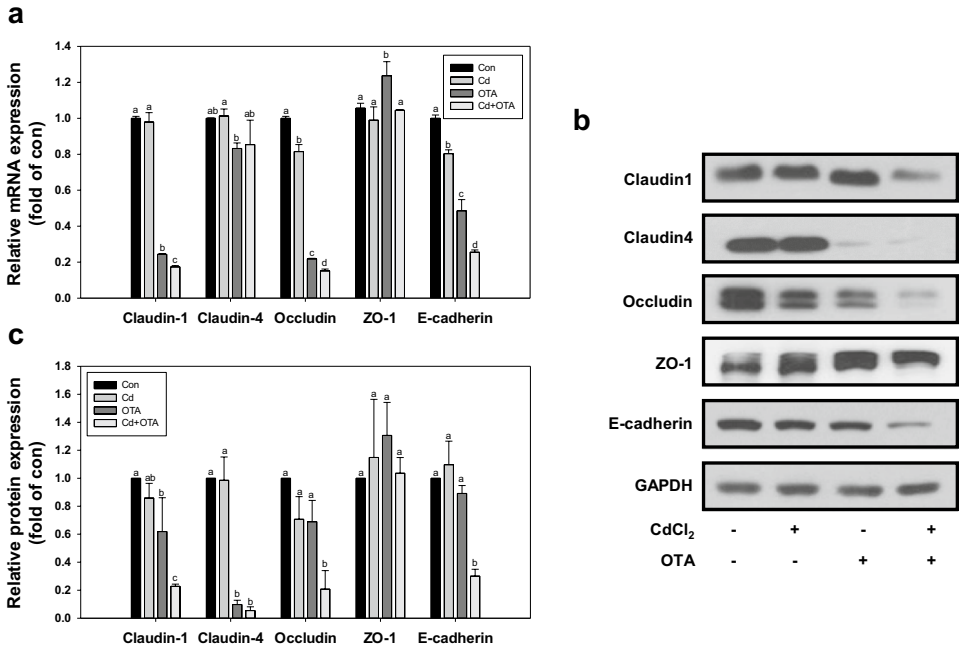

Fig. 3 Individual and combined effects of Cd and OTA on the (**a**) mRNA and (**b**, **c**) proteins expression levels of tight junction and adherent junction proteins in differentiated Caco-2 cells. Caco-2 cells were treated with $CdCl_2$ (2 µmol/L) and OTA (3 µmol/L) for 48 h. The mRNA expression levels were measured using qRT-PCR and expressed in terms of $2^{-\Delta\Delta Ct}$ values. The protein expression levels were measured using western blot. The expression levels were normalized to those of the housekeeping gene, GAPDH, and presented as fold change over the control group in terms of mean ± standard deviation of 3 independent experiments with three replicates. Different letters (**a**, **b**, **c**, and **d**) indicate significant differences in the expression levels of proteins ($p < 0.05$)

Individual and combined effects of Cd + OTA on the mRNA and protein expression of apical tight junction proteins in Caco-2 and PSI cells

In Caco-2 cells, CLDN1 and CLDN4 protein expression was significantly ($p < 0.05$) lower in Cd + OTA-treated cells, as well as in OTA-treated cells, as compared to that in Cd-treated cells (Fig. 3). In addition, the mRNA and protein expression levels of CLDN1, OCLN, and E-cadherin were significantly ($p < 0.05$) lower in Caco-2 cells treated with Cd + OTA, as compared to those in cells treated with OTA alone. In contrast, Cd and OTA treatments had less of an effect on ZO-1 mRNA and protein expression, either alone or in combination. Combined treatment of Cd + OTA in Caco-2 cells resulted in a synergistic decrease in the protein expression of E-cadherin (M = 0.989 *vs*. E = 0.300; $p < 0.05$).

As shown in Fig. 4, as compared to that in the control and single-treated cells, combined treatment with Cd + OTA led to a significant ($p < 0.05$) reduction in the mRNA and protein expression of CLDN1, OCLN, and E-cadherin in PSI cells, similar to that seen in Caco-2 cells (Fig. 4). Although the mRNA expression of CLDN4 was significantly ($p < 0.05$) higher upon single and combined treatments of Cd + OTA, as compared to that in control in PSI cells, the protein expression of CLDN4 was significantly ($p < 0.05$) lower in PSI cells treated with Cd + OTA, while there was no significant difference between OTA and Cd + OTA treatments in PSI cells. ZO-1 protein expression was significantly ($p < 0.05$) lower in cells treated with Cd + OTA than in the control cells and cells treated with Cd or OTA individually. Combined treatment with Cd + OTA in PSI cells resulted in a synergistic decrease in the protein expression of CLDN1 (M = 0.847 *vs*. E = 0.242; $p < 0.05$) and OCLN (M = 0.647 *vs*. E = 0.0.227; $p < 0.05$).

Individual and combined effects of Cd and OTA on localization of tight junction proteins in Caco-2 and PSI cells

The localization of CLDN1, OCLN, and ZO-1 was investigated to determine whether the reduction in TEER was linked to the disruption of the tight junction structure in Caco-2 cells and PSI cells (Fig. 5). In Caco-2 control cells, all of these proteins were localized to tight junctions in a "honeycomb" pattern, with only a few located in the cytoplasm (Fig. 5a). In PSI control cells, the same localization pattern of OCLN and ZO-1 proteins, aside from CLDN1, was observed (Fig. 5b). The localization patterns in Caco-2 and PSI cells exposed to Cd or OTA were comparable to those in control cells. In contrast to the control or single treatments, combined Cd + OTA treatment resulted in a redistribution of Cd + OTA into the intracellular

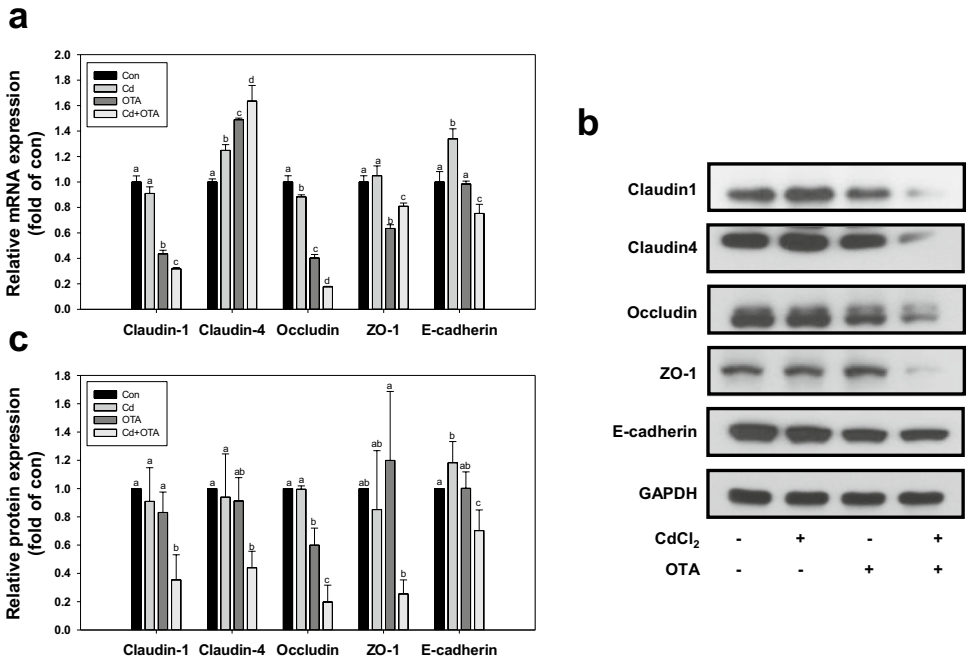

Fig. 4 Individual and combined effects of Cd and OTA on the (**a**) mRNA and (**b**, **c**) proteins expression level of tight junction and adherent junction proteins in differentiated PSI cells. PSI cells were treated with $CdCl_2$ (0.4 µmol/L) and OTA (0.6 µmol/L) for 48 h. The mRNA expression levels were measured using qRT-PCR and expressed in terms of $2^{-\Delta\Delta Ct}$ values. The protein expression levels were measured using western blot. The expression levels were normalized to those of the housekeeping gene, GAPDH, and presented as fold change over the control group in terms of mean ± standard deviation of 3 independent experiments with three replicates. Different letters (**a**, **b**, **c**, and **d**) indicate significant differences in the expression levels of proteins ($p < 0.05$)

compartment. Combined treatment with Cd + OTA caused disruption of continuity, such as a discrete punctate pattern and broken junctions, as indicated by the red arrow in Fig. 5.

Discussion

Food can be contaminated by contaminants such as mycotoxins and hazardous heavy metals. Cd is a pollutant that may enter the food chain by accumulating in plants and shellfish (Faroon et al. 2013; Kirkham 2006). OTA is a mycotoxin found in cereals, meats, cheese, dried and fresh fruits, and vegetables (CONTAM et al. 2020; Lee and Ryu 2017). Because cereals and cereal-based foods are significant sources of Cd and OTA exposure, co-contamination in meals can occur in humans (EFSA 2012; Kim et al. 2019; Kirkham 2006). Consumers may ingest more than one type of food contamination simultaneously, which presents a compelling reason to investigate the combined toxicities of different food contaminants. Several studies have monitored mycotoxins and heavy metals in cereals and cereal-based products (Kovač et al. 2021; Mosayebi and Mirzaee 2014; Yang et al. 2020). Co-exposure to patulin (a common mycotoxin) and Cd causes synergistic cytotoxicity in vitro and exacerbates liver damage in vivo (Cui et al. 2021). The synergistic toxicity caused by the co-administration of patulin and Cd is due to the enhanced generation of reactive oxygen species. In both female and male mice, co-exposure to aflatoxin B_1 and Cd exhibited an additive effect on acute oral toxicity (Zhao et al. 2019). The effects on caspase-3 activation in the MDCK-C7 canine collecting duct cell line were additive when various doses of Cd and OTA were combined (Weber et al. 2005). These data suggest that the concentration and mix of toxins used, as well as the cell line investigated, have an influence on the mechanism that leads to cellular effects.

Mean values of Cd and OTA in cereal-based products collected from Shanghai, China, in 2010 were 17.6 µg (0.157 µmol) in kg of sample and 94.2 µg (0.233 µmol) in kg of sample, respectively, with a molar ratio of Cd to OTA of 1 to 1.5 in cereal products (Yang et al. 2020). The current study employed a Cd:OTA ratio of 1:1.5, indicating a synergistic interaction utilizing the Chou and Talalay approach, based on the fa-CI plot and CI values obtained from cell viability. Caco-2 and PSI cells were treated with 2 µmol/L Cd + 3 µM OTA and 0.4 µmol/L Cd + 0.6 µM OTA, respectively, to evaluate the interactive effect of Cd + OTA. To our best knowledge, this is the first study to evaluate the single and combination effects of Cd and OTA on the intestinal barrier, using pig-derived small intestine epithelial PSI cells and human colon-derived intestinal epithelial Caco-2 cells, with a determined ratio of Cd and OTA.

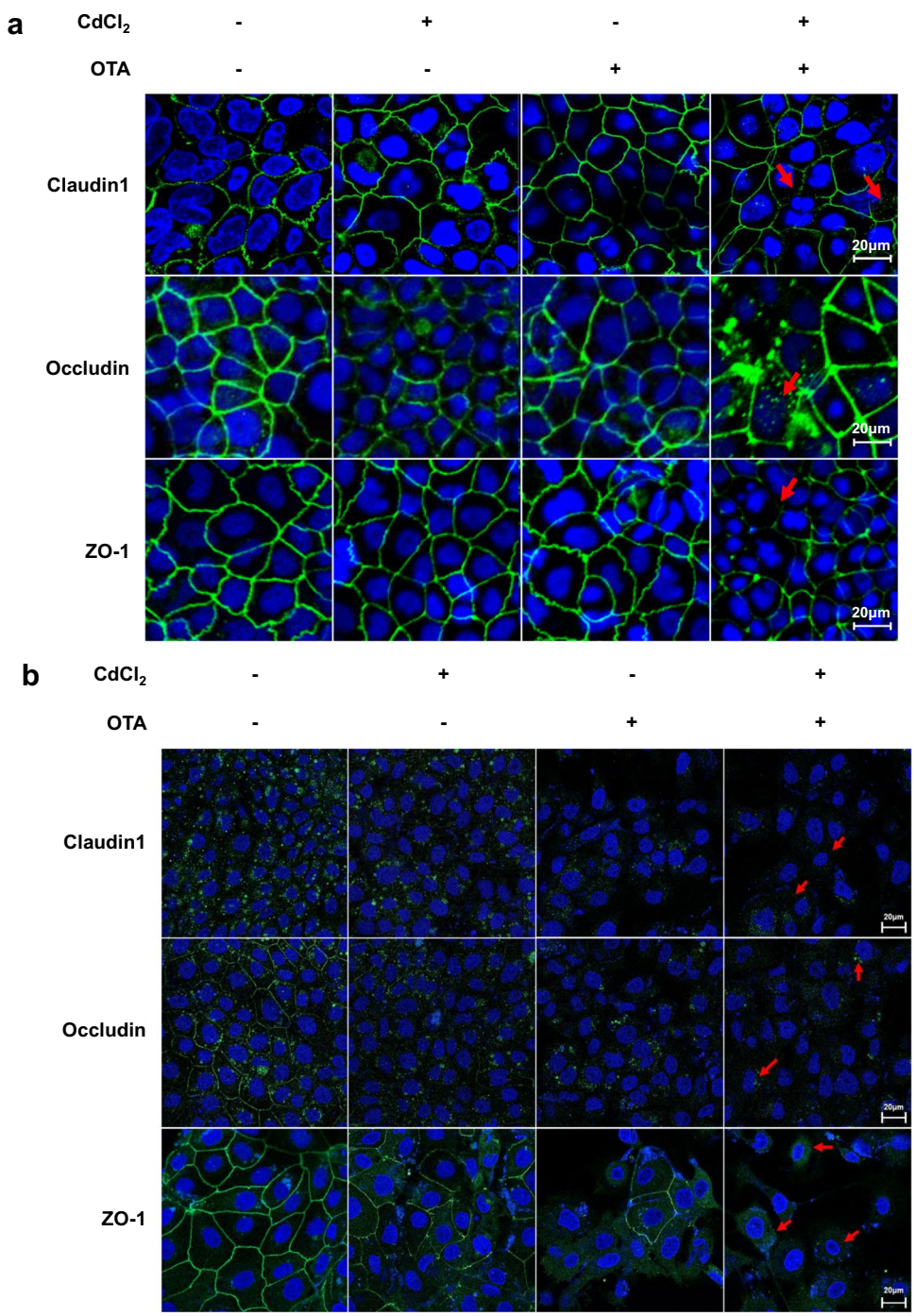

Fig. 5 Individual and combined effects of Cd and OTA on localization of tight junction proteins. Localization of the tight junction proteins was assessed using immunofluorescence in (**a**) Caco-2 cells and (**b**) PSI cells. Caco-2 cells differentiated for 21 d were treated with $CdCl_2$ (2 µmol/L) and OTA (3 µmol/L) for 48 h, while the undifferentiated PSI cells were treated with $CdCl_2$ (0.4 µmol/L) and OTA (0.6 µmol/L) for 48 h. The intercellular localization of claudin1 (green), occludin (green), ZO-1 (green), and nucleus (DAPI, blue) was measured using a confocal laser-scanning microscope, with a 20× objective and a specific antibody. Tight junction protein localization revealed a non-continuous line, due to redistribution and disruption upon co-exposure to Cd + OTA, as indicated using the red arrow

If contaminated cereal and cereal-based items are ingested and diluted with 1 L of gastrointestinal fluid in the stomach and intestines (Sergent et al. 2005), the intestinal concentrations at the maximum exposure can reach up to 2.4 µmol/L Cd and 1.4 µmol/L OTA. Therefore, the quantities employed in this study are believed to be within the range of intestinal concentrations that could be found as a result of consuming contaminated food. Caco-2 cells are frequently employed in intestinal barrier research and have morphological and biochemical features of enterocytes, such as tight junctions and specialized transport systems, following differentiation (Hidalgo et al. 1989). Tight junctions are tighter in colon-derived-Caco-2 cells than in the small intestines, suggesting that permeability may differ between the Caco-2 cell model and in vivo (Lennernäs et al. 1996).

Based on the intestinal barrier function determined in terms of TEER, Cd and OTA displayed an additive effect on paracellular permeability in Caco-2 cells, while in PSI cells, the effect was synergistic. The results demonstrated

that CLDN1, OCLN, and E-cadherin are more implicated in intestinal barrier dysfunction with Cd + OTA treatment, with E-cadherin protein expression decreasing synergistically in Caco-2 cells and CLDN1 and OCLN protein expression decreasing synergistically in PSI cells. However, the interactions and mechanisms of Cd and OTA remain unclear. In vivo and in vitro, a low dosage of arsenic was found to exacerbate the intestinal barrier dysfunction caused by deoxynivalenol, a mycotoxin (Liu et al. 2022). The authors suggested that aryl hydrocarbon receptor-mediated autophagy regulates the damage to the intestinal barrier mediated by heavy metals and mycotoxins. As various studies have shown that separate Cd and OTA treatments also promote aryl hydrocarbon receptor expression (Ge et al. 2022; Lee et al. 2018a), aryl hydrocarbon receptor signaling pathway activation may play a role in the interactive effects of Cd + OTA on the intestinal barrier dysfunction mechanism.

Our data revealed that combining Cd + OTA treatments increased the barrier dysfunction of intestinal epithelial cells, whereas individual Cd and OTA treatments had limited effects, indicating that combined Cd + OTA exposure may contribute to the development of intestinal disease. The combination treatment resulted in synergistic down-regulation of claudin-1, occludin, and E-cadherin. Further studies are required to fully comprehend the processes behind the reported combination effects; more study is required. Furthermore, the current data suggest that the combined effects of OTA + Cd may have consequences at the gut level, which should not be underestimated when assessing their risks to human health.

Supplementary Information The online version contains supplementary material available at https://doi.org/10.1007/s12550-022-00464-0.

Acknowledgements We wish to gratefully acknowledge the kind support of Professor Dr. Avrelija Cencic (deceased December 2012) for making the PSI cell line available. The authors also thank the Korea University-CJ Food Safety Center (Seoul, South Korea) for providing equipment and facilities.

Funding This research was supported by a Korea University grant (K1910641).

Data availability The data that support the findings of this study are available upon request from the corresponding author, K.-W. Lee.

Declarations

Conflict of interest The authors declare no competing interests.

References

Alizadeh A, Akbari P, Varasteh S, Braber S, Malekinejad H, Fink-Gremmels J (2019) Ochratoxin A challenges the intestinal epithelial cell integrity: results obtained in model experiments with Caco-2 cells. World Mycotoxin J 12:399–407. https://doi.org/10.3920/WMJ2019.2451

Brizio P, Benedetto A, Squadrone S, Curcio A, Pellegrino M, Ferrero M, Abete M (2016) Heavy metals and essential elements in Italian cereals. Food Addit Contam B Surveill 9:261–267. https://doi.org/10.1080/19393210.2016.1209572

Cabrera C, Ortega E, Lorenzo M-L (1998) Cadmium contamination of vegetable crops, farmlands, and irrigation waters. Rev Environ Contam Toxicol 154:55–81. https://doi.org/10.1007/978-1-4612-2208-8_2

Chou T-C (2010) Drug combination studies and their synergy quantification using the Chou-Talalay method. Cancer Res 70:440–446. https://cancerres.aacrjournals.org/content/70/2/440

Cilla A, Rodrigo MJ, Zacarías L, De Ancos B, Sánchez-Moreno C, Barberá R, Alegría A (2018) Protective effect of bioaccessible fractions of citrus fruit pulps against H_2O_2-induced oxidative stress in Caco-2 cells. Food Res Int 103:335–344. https://doi.org/10.1016/j.foodres.2017.10.066

Cui J, Yin S, Zhao C, Fan L, Hu H (2021) Combining patulin with cadmium induces enhanced hepatotoxicity and nephrotoxicity in vitro and in vivo. Toxins 13:221. https://doi.org/10.3390/toxins13030221

Duizer E, Gilde AJ, Versantvoort CH, Groten JP (1999) Effects of cadmium chloride on the paracellular barrier function of intestinal epithelial cell lines. Toxicol Appl Pharmacol 155:117–126. https://doi.org/10.1006/taap.1998.8589

European Commission (2006) Commission Regulation No 1881/2006 of 19 December 2006 Setting maximum levels for certain contaminants in foodstuffs. Off J Eur Union L 364:176. Last consolidated version available from https://eur-lex.europa.eu/legal-content/DE/AUTO/?uri=CELEX:02006R1881-20180319. Accessed 23 May 2021

EFSA (2006) Opinion of the Scientific Panel on contaminants in the food chain [CONTAM] related to ochratoxin A in food. EFSA J 4:365. https://doi.org/10.2903/j.efsa.2006.365

EFSA (2012) Cadmium dietary exposure in the European population. EFSA J 10:2551. https://doi.org/10.2903/j.efsa.2012.2551

EFSA Panel on Contaminants in the Food Chain (CONTAM), Schrenk D, Bodin L, Chipman JK, del Mazo J, Grasl-Kraupp B, Hogstrand C, Hoogenboom L, Leblanc JC, Nebbia CS, Nielsen E (2020). Risk assessment of ochratoxin A in food. EFSA J 18(5):e06113. https://doi.org/10.2903/j.efsa.2020.6113

FAO and Who (2002) Safety evaluation of certain food additives and contaminants. World Health Organization, Geneva

Faroon O, Ashizawa A, Wright S, Tucker P, Jenkins K, Ingerman L, Rudisill C (2013) Toxicological profile for cadmium. Europe PMC. https://europepmc.org/article/med/24049863. Accessed 15 Jul 2021

Ge J, Huang Y, Lv M, Zhang C, Talukder M, Li J, Li J (2022) Cadmium induced Fak-mediated anoikis activation in kidney via nuclear receptors (AHR/CAR/PXR)-mediated xenobiotic detoxification pathway. J of Inorg Biochemistry 227:111682. https://doi.org/10.1016/j.jinorgbio.2021.111682

Groschwitz KR, Hogan SP (2009) Intestinal barrier function: molecular regulation and disease pathogenesis. J Allergy Clin Immunol 124:3–20. https://doi.org/10.1016/j.jaci.2009.05.038

Hamnér K, Kirchmann H (2015) Trace element concentrations in cereal grain of long-term field trials with organic fertilizer in Sweden. Nutr Cycling Agroecosyst 103:347–358. https://doi.org/10.1007/s10705-015-9749-7

Hidalgo IJ, Raub TJ, Borchardt RT (1989) Characterization of the human colon carcinoma cell line (Caco-2) as a model system for intestinal epithelial permeability. Gastroenterology 96:736–749. https://doi.org/10.1016/S0016-5085(89)80072-1

IARC Working Group on the Evaluation of Carcinogenic Risks to Humans (1993) *Beryllium, cadmium, mercury, and exposures in the glass manufacturing industry*. International Agency for Research on Cancer. PMC7681476

Jørgensen K, Petersen A (2002) Content of ochratoxin A in paired kidney and meat samples from healthy Danish slaughter pigs. Food Addit Contam 19:562–567. https://doi.org/10.1080/02652030110113807

Kim K, Melough MM, Vance TM, Noh H, Koo SI, Chun OK (2019) Dietary cadmium intake and sources in the US. Nutrients 11:2. https://doi.org/10.3390/nu11010002

Kirkham M (2006) Cadmium in plants on polluted soils: effects of soil factors, hyperaccumulation, and amendments. Geoderma 137:19–32. https://doi.org/10.1016/j.geoderma.2006.08.024

Kovač M, Bulaić M, Jakovljević J, Nevistić A, Rot T, Kovač T, Dodlek Šarkanj I, Šarkanj B (2021) Mycotoxins, pesticide residues, and heavy metals analysis of Croatian cereals. Microorg 9:216. https://doi.org/10.3390/microorganisms9020216

Lea T (2015) Caco-2 cell line. In: Verhoeckx K, Cotter P, López-Expósito I, Kleiveland C, Lea T, Mackie A, Requena T, Swiatecka D, Wichers H (eds) The impact of food bioactives on health. Springer, Cham, pp 103–111. https://doi.org/10.1007/978-3-319-16104-4_10

Lee HJ, Pyo MC, Shin HS, Ryu D, Lee K-W (2018a) Renal toxicity through AhR, PXR, and Nrf2 signaling pathway activation of ochratoxin A-induced oxidative stress in kidney cells. Food Chem Toxicol 122:59–68. https://doi.org/10.1016/j.fct.2018.10.004

Lee HJ, Ryu D (2017) Worldwide occurrence of mycotoxins in cereals and cereal-derived food products: public health perspectives of their co-occurrence. J Agric Food Chem 65:7034–7051. https://doi.org/10.1021/acs.jafc.6b04847

Lee SG, Kim J, Park H, Holzapfel W, Lee K-W (2018b) Assessment of the effect of cooking on speciation and bioaccessibility/cellular uptake of arsenic in rice, using in vitro digestion and Caco-2 and PSI cells as model. Food Chem Toxicol 111:597–604. https://doi.org/10.1016/j.fct.2017.11.052

Lennernäs H, Palm K, Fagerholm U, Artursson P (1996) Comparison between active and passive drug transport in human intestinal epithelial (Caco-2) cells in vitro and human jejunum in vivo. Int J Pharm 127:103–107. https://doi.org/10.1016/0378-5173(95)04204-0

Li X, Yin P, Zhao L (2017) Effects of individual and combined toxicity of bisphenol A, dibutyl phthalate and cadmium on oxidative stress and genotoxicity in HepG 2 cells. Food Chem Toxicol 105:73–81. https://doi.org/10.1016/j.fct.2017.03.054

Liu S, Kang W, Mao X, Du H, Ge L, Hou L, Yuan X, Wang M, Chen X, Liu Y (2022) Low dose of arsenic exacerbates toxicity to mice and IPEC-J2 cells exposed with deoxynivalenol: aryl hydrocarbon receptor and autophagy might be novel therapeutic targets. Sci Total Environ 832:155027. https://doi.org/10.1016/j.scitotenv.2022.155027

Luissint A-C, Parkos CA, Nusrat A (2016) Inflammation and the intestinal barrier: leukocyte–epithelial cell interactions, cell junction remodeling, and mucosal repair. Gastroenterology 151:616–632. https://doi.org/10.1053/j.gastro.2016.07.008

Luo S, Terciolo C, Bracarense APF, Payros D, Pinton P, Oswald IP (2019) In vitro and in vivo effects of a mycotoxin, deoxynivalenol, and a trace metal, cadmium, alone or in a mixture on the intestinal barrier. Environ Int 132:105082. https://doi.org/10.1016/j.envint.2019.105082

McLaughlin JM, Singh BR (1999) Cadmium in soils and plants. In: S B McLaughlin MJ (ed) Developments in plant and soil sciences. Springer, Dordrecht, pp 1–9. https://doi.org/10.1007/978-94-011-4473-5_1

McLaughlin J, Padfield PJ, Burt JP, O'Neill CA (2004) Ochratoxin A increases permeability through tight junctions by removal of specific claudin isoforms. Am J Physiol Cell Physiol 287:C1412-C1417. https://doi.org/10.1152/ajpcell.00007.2004

Mosayebi M, Mirzaee H (2014) Determination of mycotoxin contamination and heavy metals in edible rice imported to Golestan Province. Iranian J Health Environ 6:503–514. https://doaj.org/article/b4aacc49ed72477aa9f6bd7ce347d05a

Norman JN (1992) Environmental health criteria 134: Cadmium. In: WHO, Geneva. pp 17–35. http://www.inchem.org/documents/ehc/ehc/ehc134.htm. Accessed 3 Nov 2020

Rana MN, Tangpong J, Rahman MM (2018) Toxicodynamics of lead, cadmium, mercury and arsenic-induced kidney toxicity and treatment strategy: a mini review. Toxicol Rep 5:704–713. https://doi.org/10.1016/j.toxrep.2018.05.012

Razzuoli E, Mignone G, Lazzara F, Vencia W, Ferraris M, Masiello L, Vivaldi B, Ferrari A, Bozzetta E, Amadori M (2018) Impact of cadmium exposure on swine enterocytes. Toxicol Lett 287:92–99. https://doi.org/10.1016/j.toxlet.2018.02.005

Romero A, Ares I, Ramos E, Castellano V, Martínez M, Martínez-Larrañaga M-R, Anadón A, Martínez M-A (2016) Mycotoxins modify the barrier function of Caco-2 cells through differential gene expression of specific claudin isoforms: protective effect of illite mineral clay. Toxicol 353:21–33. https://doi.org/10.1016/j.tox.2016.05.003

Rusanov A, Smirnova A, Poromov A, Fomicheva K, Luzgina N, Majouga A (2015) Effects of cadmium chloride on the functional state of human intestinal cells. Toxicol In Vitro 29:1006–1011. https://doi.org/10.1016/j.tiv.2015.03.018

Sergent T, Garsou S, Schaut A, De Saeger S, Pussemier L, Van Peteghem C, Larondelle Y, Schneider Y-J (2005) Differential modulation of ochratoxin A absorption across Caco-2 cells by dietary polyphenols, used at realistic intestinal concentrations. Toxicol Lett 159:60–70. https://doi.org/10.1016/j.toxlet.2005.04.013

Skendi A, Papageorgiou M, Irakli M, Katsantonis D (2019) Presence of mycotoxins, heavy metals and nitrate residues in organic commercial cereal-based foods sold in the Greek market. JCF 15:1–11. https://doi.org/10.1007/s00003-019-01231-7

Tinkov AA, Gritsenko VA, Skalnaya MG, Cherkasov SV, Aaseth J, Skalny AV (2018) Gut as a target for cadmium toxicity. Environ Pollut 235:429–434. https://doi.org/10.1016/j.envpol.2017.12.114

Trapecar M, Cencic A (2012) Application of gut cell models for toxicological and bioactivity studies of functional and novel foods. Foods 1:40-51. https://doi.org/10.3390/foods1010040

Wang H, Zhai N, Chen Y, Fu C, Huang K (2018) OTA induces intestinal epithelial barrier dysfunction and tight junction disruption in IPEC-J2 cells through ROS/Ca2+-mediated MLCK activation. Environ Pollut 242:106–112. https://doi.org/10.1016/j.envpol.2018.06.062

Wang P, Chen H, Kopittke PM, Zhao F-J (2019) Cadmium contamination in agricultural soils of China and the impact on food safety. Environ Pollut 249:1038–1048. https://doi.org/10.1016/j.envpol.2019.03.063

Weber F, Freudinger R, Schwerdt G, Gekle M (2005) A rapid screening method to test apoptotic synergisms of ochratoxin A with other nephrotoxic substances. Toxicol In Vitro 19:135–143. https://doi.org/10.1016/j.tiv.2004.08.002

WHO and IARC (1993) Some naturally occurring substances: food items and constituents, heterocyclic aromatic amines and mycotoxins. In: IARC monographs on the evaluation of the carcinogenic risk of chemicals to humans, Vol. 56. International Agency for Research on Cancer, Lyon, pp 599. https://publications.iarc.fr/74

Yang X, Zhao Z, Tan Y, Chen B, Zhou C, Wu A (2020) Risk profiling of exposures to multiclass contaminants through cereals and cereal-based products consumption: a case study for the

inhabitants in Shanghai, China. Food Control 109:106964. https://doi.org/10.1016/j.foodcont.2019.106964

Zhai Q, Tian F, Zhao J, Zhang H, Narbad A, Chen W (2016) Oral administration of probiotics inhibits absorption of the heavy metal cadmium by protecting the intestinal barrier. Appl Environ Microbiol 82:4429–4440. https://doi.org/10.1128/AEM.00695-16

Zhao Q, Yang Z-S, Cao S-J, Chang Y-F, Cao Y-Q, Li J-B, Yao Z-X, Wen Y-P, Huang X-B, Wu R (2019) Acute oral toxicity test and assessment of combined toxicity of cadmium and aflatoxin B1 in kunming mice. Food Chem Toxicol 131:110577. https://doi.org/10.1016/j.fct.2019.110577